Extratropical Conferenc

THE COLORADO FRONT RANGE BLIZZARD OF 1990: THE STRUCTURE AND EVOLUTION OF A SMALL-SCALE OCCLUDED FRONT

Roy Rasmussen, Jon Reisner

Greg Stossmeister

National Center for Atmospheric Research
Boulder, Colorado

1. INTRODUCTION

In the Norwegian model for cyclone development an occlusion is a process in which a cold front overtakes a warm front. The exact nature of this process, however, has been questioned by a number of authors (see Schultz and Mass, 1993 for an overview) leading to the development of a variety of conceptual models. So far, the main limitation in determining the validity of any one of the proposed conceptual models has been the lack of detailed observations (Schultz and Mass, 1993). Though the exact details of the occlusion process are unclear, the scale on which it can occur ranges anywhere from that of a supercell thunderstorm (Lemone and Doswell, 1979) to that of a large-scale cyclone (Reed et al., 1994).

An occlusion usually occurs during the mature part of a system's development. During this time the forward progress of the system typically begins to slow down. The combination of surface convergence provided by the occlusion, the possible presence of convective instability, and the slow movement of the parent system sets the stage for repeated convective development over a localized area and the potential for flash flooding or heavy snow. Additionally, if an occlusion occurred in the vicinity of complex terrain (e.g., Colorado Rockies) additional lift could be provided by the terrain.

In this paper we will examine a rather small-scale occlusion ($Ro \approx 1$) which appeared to be responsible for a strong but narrow band of convection in the vicinity of the Front Range of northeast Colorado during the afternoon of the 6 March 1990. Section 2 will provide a brief summary of the observation network used to document the storm's evolution. Section 3 will give a short summary of the storm and a discussion of the observations. Section 4 will overview the numerical model used to simulate the occlusion process. Section 5 will present results from the numerical simulations and Section 6 will offer some concluding remarks.

* NCAR is sponsored by the National Science Foundation.

2. DESCRIPTION OF DATASET

The observational data used in this study was collected during the 1990 Winter Icing and Storms Project (WISP90) which took place over northeastern Colorado between 1 February 1990 and 31 March 1990. The primary goals of the project were to improve the understanding of processes involved in the production and depletion of supercooled liquid water and to understand the dynamics of winter storms. During WISP90 the instrumentation network (Fig. 1) included 2 Doppler radars, 19 Portable Automated Mesonet (PAM II) stations, 22 Program for Regional Observing and Forecasting Systems (PROFS) mesonet stations, 3 dual-channel microwave radiometers, and 2 wind profilers (see Rasmussen et al., 1992, for a detailed description).

3. STORM OVERVIEW AND OBSERVATIONS

During 5-7 March 1990, a blizzard occurred along the Colorado Front Range during which 25-86 cm of snow fell along a 60 km wide corridor extending from Cheyenne, Wyoming to the north, to Colorado Springs, Colorado to the south. The strong winds and heavy snowfall associated with the blizzard were produced as a result of a deep cutoff cyclonic system that developed in the Four Corners area of the southwestern United States. The synoptic structure of this storm was discussed by Marwitz and Toth (1993) and shown to be similar to the frontal-fracture conceptual model of cyclone evolution discussed by Shapiro and Keyser (1990), with a cold front propagating ahead of the surface low, and moisture wrapping around the northeast quadrant of the low. Figure 2a shows the cloud structure associated with this storm during its mature stage.

During the main part of the storm, moist easterly upslope flow occurred along the Front Range from the surface to 250 hPa, resulting in heavy precipitation for a period of approximately 36 hours. The distribution of precipitation in this storm showed a strong dependence on mesoscale features. Three major features were responsible for focussing the heavy snow along the Colorado Front Range: a

barrier-parallel low-level northerly jet, a dry intrusion, and a small scale occlusion (Fig. 2b). The development of the barrier jet has been discussed by Marwitz and Toth (1993). Stossmeister and Rasmussen (1992) discussed the formation of convection along the dry intrusion. They showed that the eastern edge of the dry intrusion was associated with convective development, and had characteristics similar to a dry line. This paper will discuss the mesoscale structure and evolution of a small scale occlusion that formed as the northern and southern boundaries of the dry intrusion approached each other.

The dry intrusion at the surface is shown in Fig. 3a during the mature stage of the storm as a plume of potentially warmer air contained within the 310° K equivalent potential temperature contour. Also evident in this figure is the plume of colder air associated with the barrier jet located near the foothills.

A radar image (Fig. 3b) at 2100 UTC, 6 March shows that convective development was present along the northern portion of the dry intrusion. In fact, most of the precipitation that fell over the Front Range during the afternoon of 6 March can be attributed to convective elements which formed along and to the north of this boundary and then translated back towards the Front Range (Stossmeister and Rasmussen, 1992).

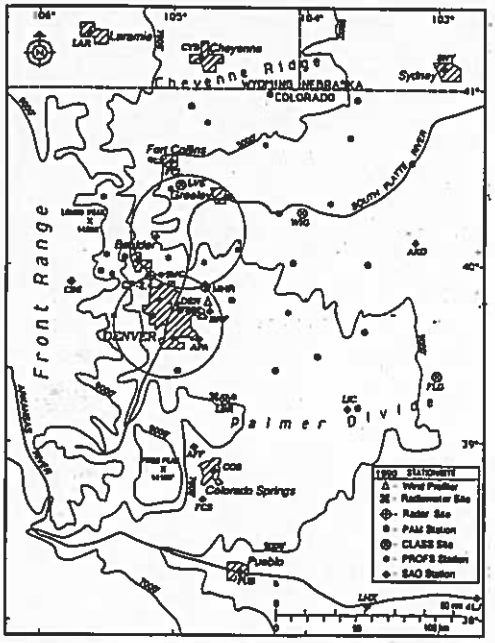

Fig. 1 *Winter Icing and Storms Project (WISP90) network of instruments showing the location of the Doppler radars, CLASS sounding stations, PAM and PROFS mesonet stations, radiometer sites, wind profiler sites, and SAO stations. Topographic contours are given every 2000 ft. The shaded region represents terrain above 9000 ft.*

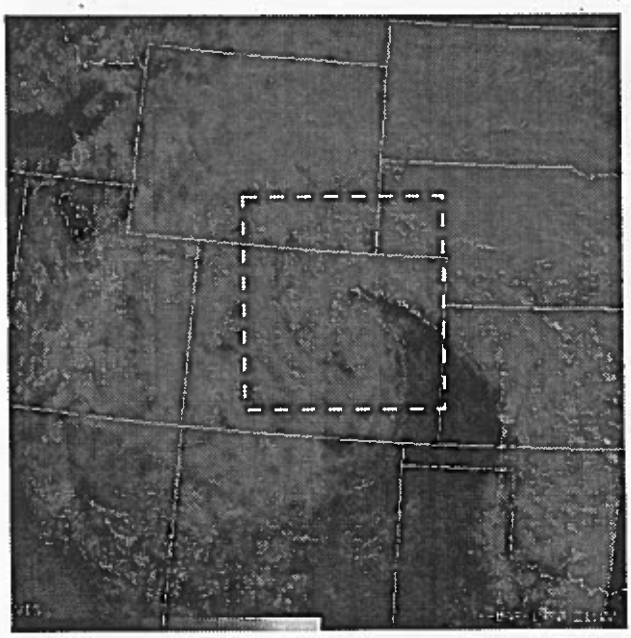

Fig. 2a. *Regional visible satellite image of the storm at 2100 UTC, 6 March 1990. State boundaries are given by the solid lines with Colorado in the center. The dashed box indicates the domain of the visible satellite image in Fig. 2b.*

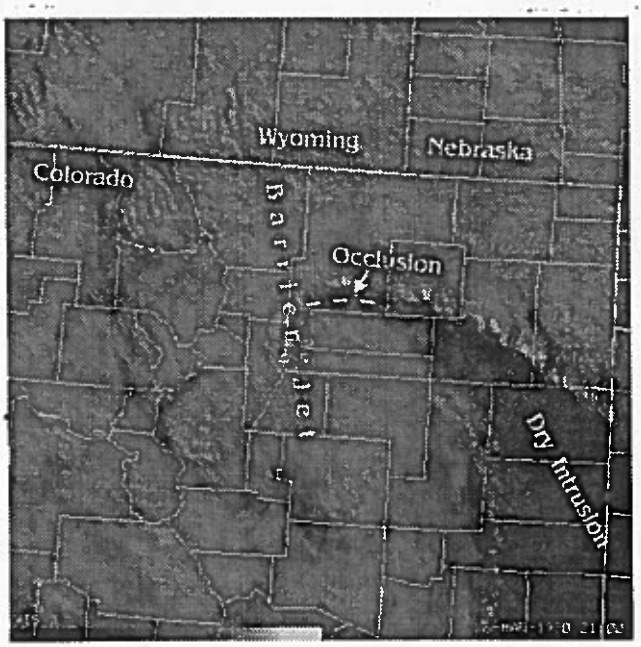

Fig. 2b. *Visible satellite image at 2100 UTC, 6 March 1990 within the domain indicated by the dashed box in Fig. 2a. Also indicated are the locations of the barrier jet, the dry intrusion, and the occlusion. County boundaries are also given.*

After 2100 UTC 6 March the western portion of the southern boundary of the dry intrusion began to surge towards the north while, in response to northerly flow along the Front Range, the western portion of the northern boundary of the dry intrusion progressed slowly towards the south-southwest. (Fig. 7; note the evolution of the $\theta_e = 306$ contour.) As could be expected, the two boundaries eventually collided ($\approx$ 2200 UTC, 6 March) resulting in the formation of a single frontal boundary, or as will later be shown, an occluded front. As can be seen in Fig. 4b an east-west convective line has developed at a location just northeast of Denver shortly after this time. The contours of θ_e at 2300 UTC show rapid collapse in the region northeast of Denver (Fig. 4a), suggesting a single frontal surface at that time.

Radar images between 2300 UTC and 0000 UTC show that the convective band essentially remained stationary until its dissipation around 0000 UTC. Since the location of the presumed front is not well resolved by the θ_e analysis, uncertainty exists as to the actual existance of an occluded front, the strength of the front, and the spatial dimensions of the front. To help address these uncertainties a high-resolution numerical simulation of the occlusion process was conducted.

4. MODEL DESCRIPTION AND SETUP

The mesoscale model used to simulate the small-scale occlusion was a nonhydrostatic extension (hereafter referred to as MM5) of the hydrostatic model (previously referred to as MM4) presented by Anthes and Warner (1978). MM5 can accommodate four-dimensional data assimilation, multi-nested domains, and various physical parameterizations (Grell et al., 1994). The domain was initialized with data obtained from an analysis package that incorporates raw upper-air, surface data, and/or data from other numerical weather prediction models and interpolates the data to the chosen grid (Manning and Haagenson, 1994).

In the simulation of this winter storm four domains of horizontal resolution 60.0 km, 20.0 km, 6.7 km, and 2.2 km were run (see Fig. 5 for location of the nests). The 20.0 km domain was run concurrently with the 60.0 km domain; whereas, the 6.7 and 2.2 km domains were run in a one-way nest mode. Initial and boundary data for the 60.0 km domain were supplied from NMC archived fields. Initial and boundary conditions for the 2.2 and 6.7 km domains were interpolated from results from the 6.7 and 20.0 km domains. The 60 and 20 km domains were run between 1200 UTC, 5 March and 0000 UTC, 7 March. The 6 and 2 km domains were run between 1500/1800 UTC, 6 March and 0000 UTC, 7 March.

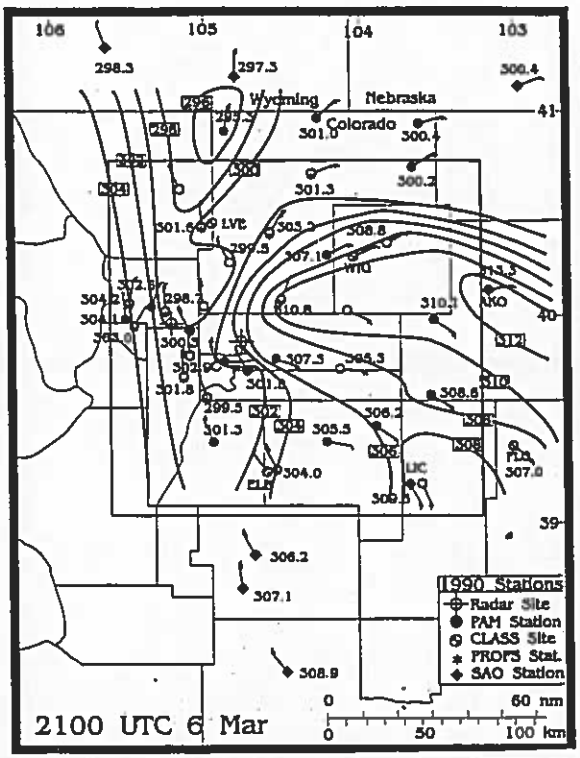

Fig. 3a. *Surface θ_e analysis at 2100 UTC, 6 March 1990. Contour interval is 2°K. Also shown are wind barbs at the SAO and mesonet stations with a long flag indicating 5 m s^{-1} and a short flag 2.5 m s^{-1}. Outlined box indicates the domain of the radar plots in Figs. 3b and 4b and model output in Figs. 6 and 7.*

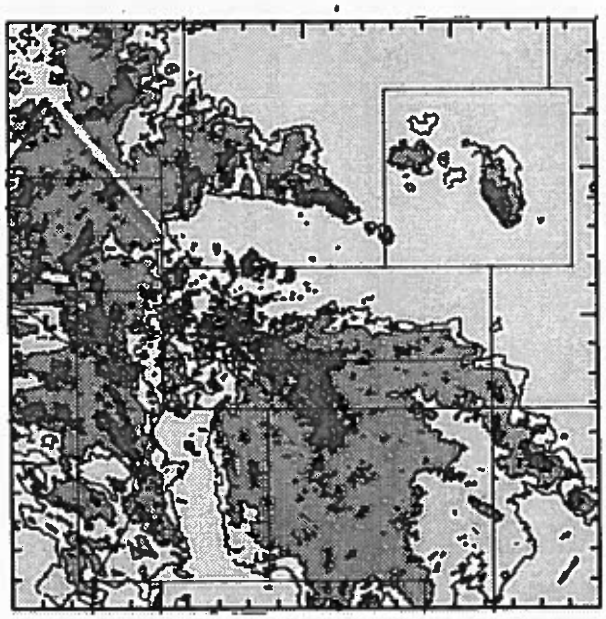

Fig. 3b. *Radar reflectivity (dBZ) from Mile High Radar from a 0.8° PPI at 2056 UTC, 6 March 1990. Contours are 0, 10, 20 and 30 dBZ. The distance between tick marks is 10 km.*

Vertical resolution was the same for all domains with 27 vertical levels at σ = t.025, 0.07, 0.11, 0.15, 0.19, 0.23, 0.27, 0.31, 0.35, 0.39, 0.43, 0.51, 0.59, 0.63, 0.71, 0.75, 0.79, 0.83, 0.87, 0.91, 0.945, 0.97, 0.985 and 0.995. Time steps were chosen to be 180 s, 60 s, 20 s , and 10 s for the 60, 20, 6.7, and 2.2 km grids respectively.

For all simulations the model was run with the following physical parameterizations activated: a high-resolution planetary boundary layer scheme (Zhang and Anthes, 1982), the cumulus parameterization scheme of Grell et al. (1991), a surface radiation budget, an upper radiative boundary condition (Grell et al., 1994), and the microphysical option as described by Reisner et al. (1993).

5. RESULTS

In the following we present results from the 2.2 km domain during the mature stage of the storm. After 3 h of model integration, the simulated θ_e (Fig. 6 and compare with boxed area of Fig. 3a) field agrees fairly well with the observed θ_e field at 2100 UTC, 6 March. As in the observed field, highest values of θ_e are found in the dry intrusion with a decrease in θ_e to the north/south of the intrusion. The intensity and location of the barrier jet are also well simulated by the model, as evident in Fig. 6.

The formation of the convective line at 2300 UTC as observed in the radar data was well simulated by the model. Examination of the model output shows that the convective line forms as a result of the western portion of the southern boundary of the dry intrusion rapidly moving northward overtaking the northern dry intrusion boundary (Fig. 7a). This results in the formation of a small scale occluded front. Solenoidal circulations along the occluded front are quite strong leading to a narrow strip of strong ascent which is in approximately the same location as the convective line observed by radar (compare Fig. 7b with Fig. 4b). The depth of the occluded front is quite shallow (Fig. 8a, $\approx$ 500 m) with the front having the appearance of a density current; however, upward motions at the leading edge of the front extend to a depth of $\approx$ 6 km (Fig. 8b). Since development of the shallow cold pool was associated with convection developing on the southern boundary of the dry occlusion, we believe that evaporative cooling and/or melting played a part in its formation.

6. CONCLUSIONS

Radar, surface observations, and satellite images obtained during WISP90 were used to document both the formation and evolution of what appears to be a small-scale convective line. Model simulations of this event show that the line formed during an occlusion process in which the southern boundary of a dry intrusion overtook the northern boundary, resulting in a concentrated region of uplift and convective development. Since the horizontal vorticity across the front was due to horizontal gradients in bouyancy and not vertical wind shear, we believe that the occluded front can best be described as a "surge-occlusion".

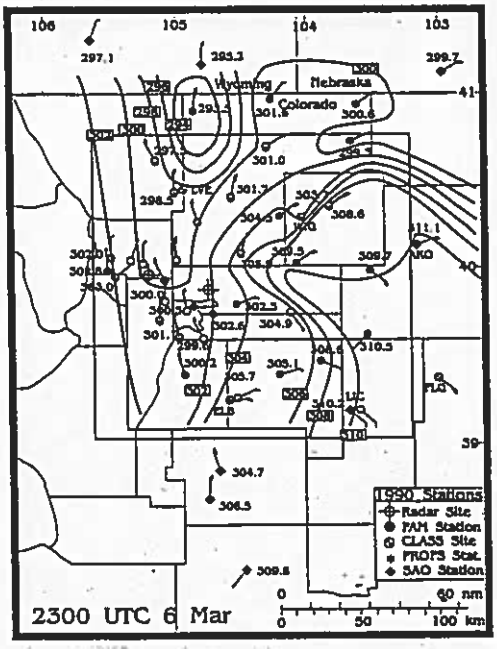

Fig. 4a. Same as Fig. 3a except at 2300 UTC, 6 March 1990.

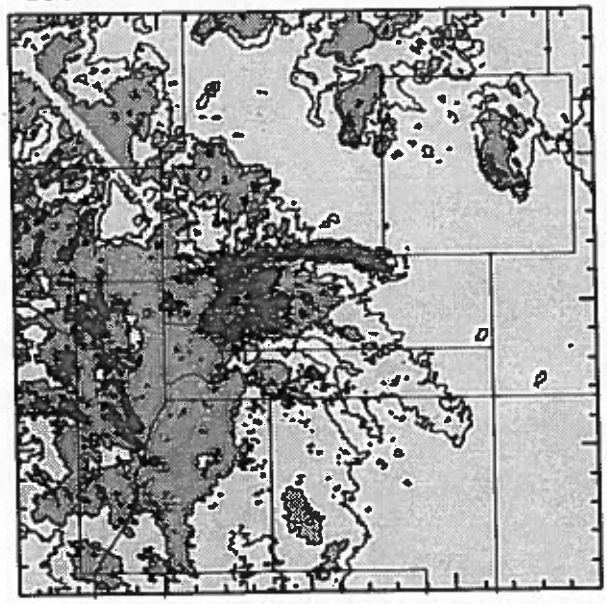

Fig. 4b. *Same as Fig. 3b except at 2300 UTC, 6 March 1990.*

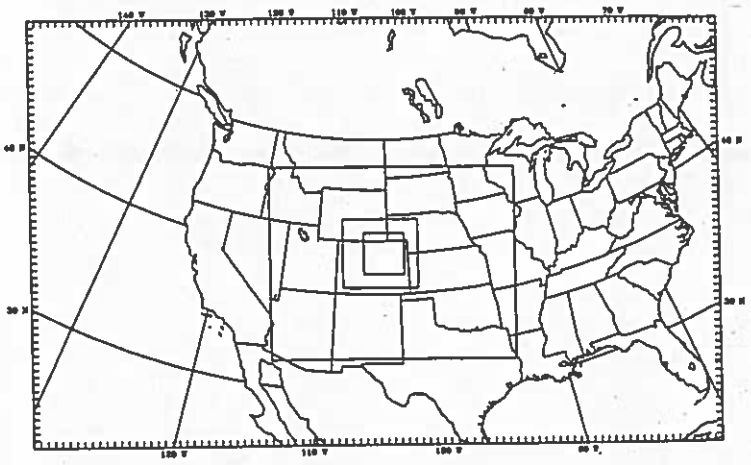

Fig. 5. *Location of the four model nests.*

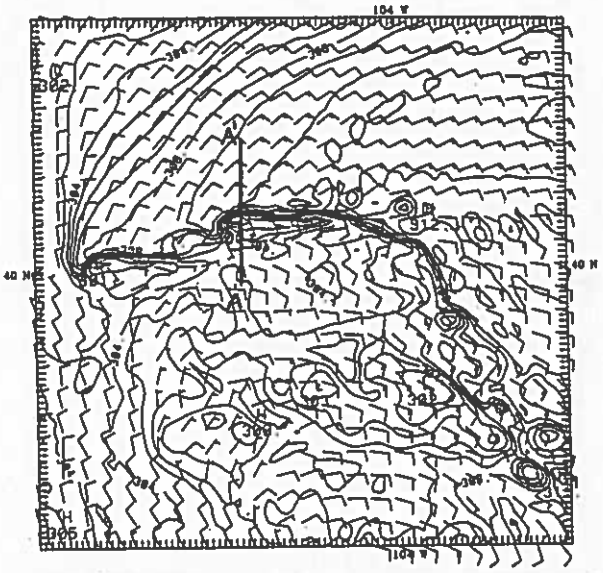

Fig. 7a. *Same as Fig. 6 except at 2300 UTC. Thick line indicates the location of the vertical section in Figs. 8a and b.*

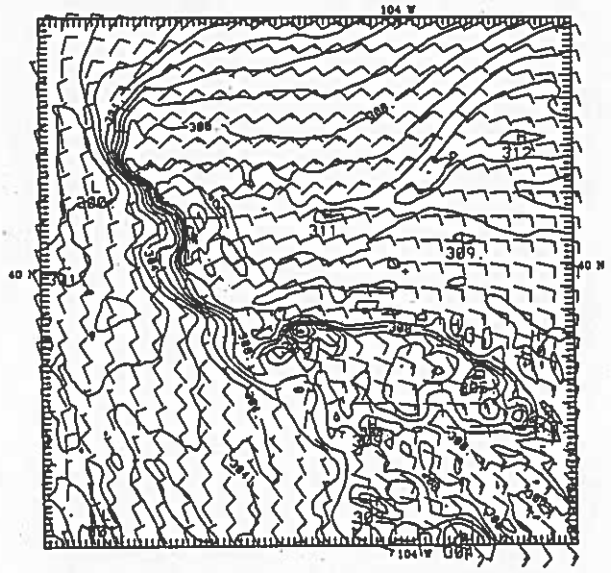

Fig. 6. *Equivalent potential temperature contours and wind barbs from the* $\sigma = 0.995$ *level of the model at 2100 UTC, 6 March 1990. Contours are given every 1°K. The domain is the same physical space as the radar reflectivity domain in Figs. 3b and 4b. Tick marks are every 2.2 km. Full barb is 10 m* s^{-1}*. Half barb is 5 m* s^{-1}*. Wind barbs are plotted every 4th grid point.*

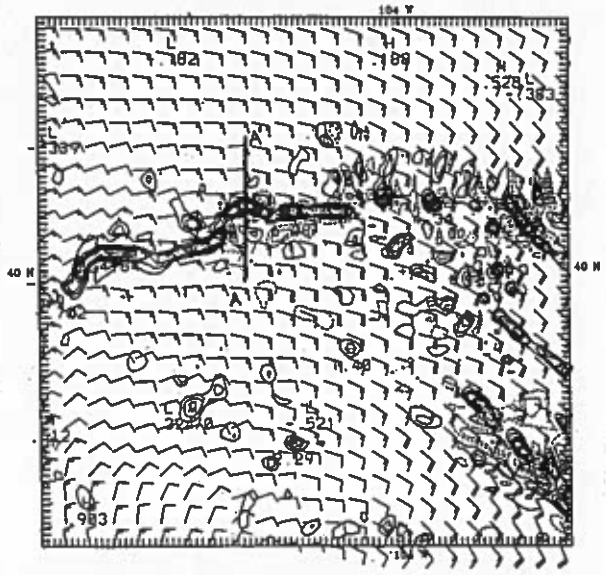

Fig. 7b. *Same as Fig. 7a except for vertical velocity. Contour interval is 0.5 m* s^{-1}*. Thick line indicates the location of the vertical section in Figs. 8a and 8b.*

7. ACKNOWLDGEMENTS

This research is sponsored by the National Science Foundation through an Interagency Agreement in response to requirements and funding by the Federal Aviation Administration's Aviation Weather Development Program. The authors also

acknowledge Carol Makowski for typing and formatting the manuscript.

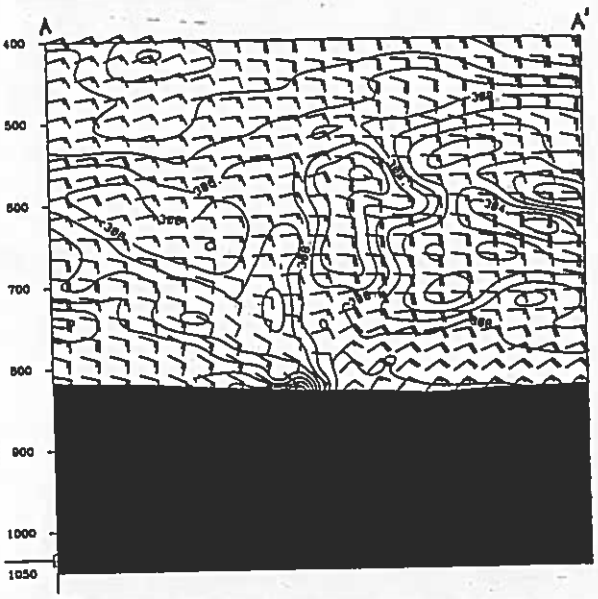

Fig. 8a. *Vertical section of θ_e at 2300 UTC from the model along the thick line shown in Fig. 7. Contour interval is 1°K. Wind barbs are for horizontal flow and have the same convention as in Fig. 6.*

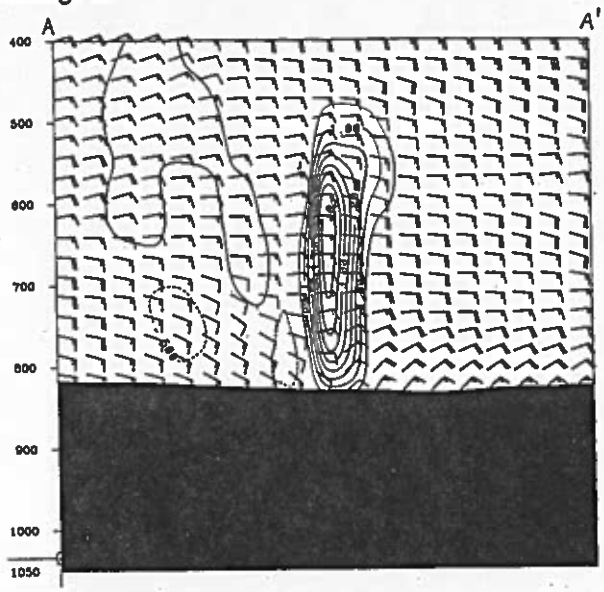

Fig. 8b. *Same as Fig. 8a except for vertical velocity. Contour interval is 0.5 m s^{-1}.*

8. REFERENCES

Anthes, R.A. and T.T. Warner, 1978: Development of hydrodynamical models suitable for air pollution and other mesometeorological studies. *Mon. Wea. Rev.*, **106**, 1045–1078.

Grell, G.A., Y.H. Kou and R. Pasch, 1991: Semi-prognostic tests of cumulus parameterisation schemes in the middle latitudes. *Mon. Wea. Rev.*, **119**, 5–31.

Grell, G.A., J. Dudhia and D.R. Stauffer, 1994: *A description of the Fifth-Generation Penn State/NCAR Mesoscale Model (MM5).* NCAR/TN-398+IA, National Center for Atmospheric Research, CO, 107 pp.

Lemone, L.R. and C.R. Doswell III, 1979: Severe thunderstorm evolution and mesocyclone structure as related to tornadogenesis. *Mon. Wea. Rev.*, **107**, 1184–1197.

Manning, K.W. and P.L. Haagenson: *Data ingest and objective analysis for the PSU/NCAR modeling system: Programs* **DATAGRID** *and* **RAWINS.** NCAR/TN-376+IA, National Center for Atmospheric Research, CO, 209 pp.

Marwitz, J. and J. Toth, 1993: The Front Range blizzard of 1990. Part I: Synoptic and mesoscale structure. *Mon. Wea. Rev.*, **121**, 402–415.

Rasmussen, R.M., M.K. Politovich, J. Marwitz, W. Sand, J. McGinley, J. Smart, R. Pielke, S. Rutledge, D. Wesley, G. Stossmeister, B. Bernstein, K. Elmore, N. Powell, E. Westwater, B.B. Stankov and D. Burrows, 1992: Winter Icing and Storms Project (WISP). *Bull. Amer. Meteor. Soc.*, **73**, No. 7, 951–974.

Reisner, J.; R.T. Bruintjes and R.M. Rasmussen, 1993: Preliminary comparisons between MM5 NCAR/Penn State model generated icing forecasts and observations. *Preprints, 5th Int'l Conf. on Aviation Wea. Systems*, Vienna, VA, 2–6 August. Amer. Meteor. Soc., Boston, 65-69.

Reed, J., Y.H. Kou and S. Low-Nam, 1994: A near-adiabatic simulation of the ERICA IOP4 storm. submitted to *Mon. Wea. Rev.*

Schultz, D.M. and C.F. Mass, 1993: The occlusion process in a midlatitude cyclone over land. *Mon. Wea. Rev.*, **4**, 918–940.

Shapiro, M. and D. Keyser, 1990: Fronts, jet streams and the tropopause. *Extratropical Cyclones*, C. Newton and E. Holopainen, Eds., Amer. Meteor. Soc., Boston, 167–191.

Stossmeister, G.J. and R.M. Rasmussen, 1992: Precipitation band structure in the Front Range blizzard of March 5-7, 1990. *Proceedings, 11th Int'l Conf. on Clouds and Precip.*, August. Amer. Meteor. Soc., Boston, 632–635.

Zhang, D.L. and R. L. Anthes, 1982: A high-resolution model of the planetary boundary layer-sensitivity tests and comparisons with SESAME-79 data. *J. Appl. Meteor.*, **21**, 1594–1609.